CrystEngComm

Modulation of Crystal Growth and Structure within Cerium-Based Metal–Organic Frameworks

Journal:	*CrystEngComm*
Manuscript ID	CE-ART-08-2020-001223.R1
Article Type:	Paper
Date Submitted by the Author:	31-Oct-2020

Complete List of Authors:	Wasson, Megan; Northwestern University, Otake, Ken-ichi; Kyoto University, Institute for integrated Cell-Materials Science (iCeMS) Gong, Xinyi; Northwestern University, Chemistry Strathman, Annabella; Northwestern University Islamoglu, Timur; Northwestern University, Department of Chemistry Gianneschi, Nathan; Northwestern University, Chemistry; University of California, San Diego, Chemistry and Biochemistry Farha, Omar; Northwestern University, Department of Chemistry

Modulation of Crystal Growth and Structure within Cerium-Based Metal–Organic Frameworks

Megan C. Wasson, Ken-ichi Otake, Xinyi Gong, Annabella R. Strathman, Timur Islamoglu, Nathan C. Gianneschi, and Omar K. Farha*

Affiliation: International Institute for Nanotechnology and Department of Chemistry, Northwestern University, 2145 Sheridan Road, Evanston, Illinois 60208, United States

Abstract: The intriguing catalytic properties of cerium-based materials has motivated the development of Ce-based metal–organic frameworks (MOFs). However, the controlled crystallization of Ce MOFs remains nascent due to complications with the high reductive potential of Ce^{4+} species. Modulators offer a route in other well-studied coordination networks to slow down crystallization processes to allow for corrective, uniform crystal growth. Herein, we report an investigation of modulator identity and concentration on the synthesis of a Ce-UiO-type MOF with 2,6-naphthalenedicarboxylic acid (NDC) as a linker. At low concentrations using both benzoic acid and trifluoroacetic acid, we observed a mononuclear Ce^{3+} MOF (NU-350) through single-crystal X-ray diffraction studies. Higher modulator concentrations yielded pure-phase Ce-UiO-NDC, with uniform particle sizes observed with utilizing benzoic acid as a modulator. Moreover, we demonstrated the transferability of this synthesis through the pure-phase synthesis of Ce-UiO-66 with benzoic acid as a modulator. High-resolution transmission electron microscopy observed a single crystalline domain within Ce-UiO-NDC.

Introduction

The bottom up construction of sophisticated, uniform materials from simple nano-sized building blocks has received substantial attention of the past two decades.[1,2] As atomically precise, hybrid, nanoporous materials, metal–organic frameworks (MOFs) have emerged at the forefront

of such impactful nanomaterials.[3] MOFs are composed of inorganic nodes and multidentate organic linkers that assemble into multidimensional lattices through coordination bonds.[4] As such, the frameworks access innumerable chemical functionalities to form highly tailorable structures. MOFs have been implemented in heterogeneous catalysis[5–7], water purification[8,9], drug delivery[10,11], gas capture/storage/separation[4,12–14], and chemical sensing[15–18] due to the high density of spatially isolated binding sites at nodes and linkers. MOFs have been exceptionally impactful as catalyst supports due to their crystallinity and uniformity, critical for precise identification of catalytic active sites to inform next-generation catalyst design.[19]

Earliest MOFs were based on divalent metals, namely, Zn^{2+} and Cu^{2+} and carboxylate linkers.[4,20] However, a higher charge density at the metal node was accessed with higher valent metals (Zr^{4+}, Hf^{4+}, Ce^{4+}) which subsequently increased the strength of the metal-carboxylate bond.[21–24] Of these metals, Zr^{4+}-O based frameworks have emerged as the most well-studied tetravalent species since their first inception in 2008.[21,25–31] However, strong Zr^{4+}-O bonds often yield polycrystalline materials rather than a single crystalline domain due to the fast precipitation events that occur. Additives, referred to as modulators, were discovered as a strategy to realize diffraction-quality crystals of a Zr^{4+} MOF.[32] Such modulators feature identical monotopic functionality to the multitopic linker in solution and subsequently compete with the linker through transient node binding to slow down coordination binding events.[33] Their role has been investigated throughout Zr-MOF syntheses, yet few generalizable modulation rules exist.[34–39]

Enabled by fundamental advancements in Zr^{4+} MOF syntheses, initial research toward the development of spatially isolated, periodic Ce^{4+} oxo frameworks emerged, partly inspired by the utility of its parent metal oxide within heterogeneous catalysis.[24,40,41] However, the high reductive potential of Ce^{4+} complicates the synthesis of crystalline cerium materials, including MOFs. MOF

syntheses typically rely on high boiling point, formamide-based solvents, generally dimethylformamide (DMF), under high temperatures. The *in-situ* decomposition into formic acid and dimethylamine often enables the facile formation of $Ce(HCOO)_3$ rather than an assembly of hexanuclear Ce^{4+} nodes as observed by Reinsch and team.[24,42]

Stock and coworkers first synthesized Ce^{4+} MOFs through a clever, fast precipitation strategy to access the frameworks in less than 15 minutes, prior to formation of deleterious $Ce(HCOO)_3$.[24,40] However, such methodologies sacrifice control over defect concentration, crystallite morphology, or particle size. Inconsistent particle size imparts diffusion effects, indiscernible morphology complicates identification of pure-phase materials, and defective sites, or exposed open metal sites due to missing linkers or nodes, result in vast differences in framework reactivity.[43,44] Moreover, efforts to develop controlled crystal growth processes coincide with emerging structural and mechanical characterizations which require access to well-defined surface structures (facets and edges), such as high-resolution transmission electron microscopy (HRTEM) and nanoindentation studies.[45,46]

An environmentally friendly synthesis utilized solvent free conditions to synthesize an array of Ce-UiO type MOFs, yet the mechanochemistry crystallization process precluded the formation of the characteristic octahedral morphology.[47] Previously inaccessible redox active porphyrin and pyrene – based Ce MOFs were synthesized utilizing a glycine-capped Ce^{4+} cluster which lowered the Ce reductive potential.[48,49] However, this procedure still utilizes a rapid precipitation method that prevents a controlled crystallization process. Recent work utilized a syringe-pump to slowly introduce cerium ammonium nitrate in the presence of acetic acid as a modulator to form well defined Ce-UiO-66 particles.[50] However, the practical limitations of introducing additional equipment may limit the scale of this procedure. More recently, Huang and co-workers varied

acetic acid modulator concentration and temperature to access uniform octahedral Ce-UiO-66 particles effective in the separation of CO_2 and CH_4.[51]

Toward developing Ce MOF syntheses, we elected to study the role of modulator identity and concentration on the crystal growth of Ce UiO-type frameworks. Well-reported examples within Zr MOFs include the modulator dependence on framework topology, beyond merely particle size or morphology, highlighting the potential influence these species can play in MOF syntheses.[34,52] We conducted a systematic study investigating two different modulators, benzoic acid and trifluoroacetic acid, on the controlled crystallization of a UiO Type MOF: Ce-UiO-NDC (NDC = 2,6-naphthalenedicarboxylic acid). We elected to study Ce-UiO-NDC given its higher porosity and stability toward activation procedures than the well-studied Ce-UiO-66.[53] Through varying modulator concentration, we identified two pure-phase products: Ce-UiO-NDC and NU-350, a mononuclear Ce chain MOF linked through NDC linkers. Specifically, an increase in modulator concentration resulted in both pure-phase Ce-UiO-NDC as well as large particle sizes, with benzoic acid providing high uniformity. Modulator trends developed within Ce-UiO-NDC

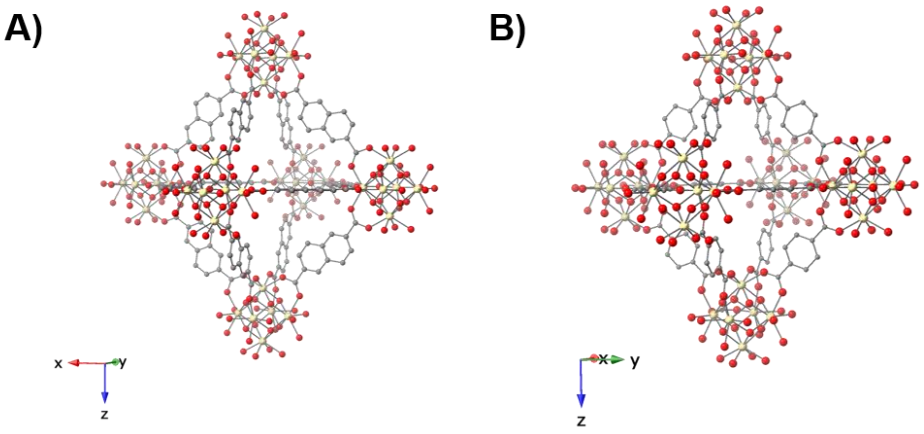

Figure 1. Structures of Ce-UiO-NDC (A) and Ce-UiO-66 (B). C, grey; O, red; Ce, pale yellow. H atoms are omitted for clarity.

were transferable for the synthesis of pure-phase octahedral Ce-UiO-66 particles. HRTEM identified a single crystalline domain within Ce-UiO-NDC.

Results and Discussion

To probe the modulator effect on the synthesis of Ce-UiO-type frameworks, we selected benzoic acid and trifluoroacetic acid (TFA), species successfully employed as modulators in the synthesis of Zr-based MOFs. We elected to first investigate Ce-UiO-NDC, a 12-connected framework based on 2,6-naphthalenedicarboxylic acid linkers that crystallizes in **fcu** topology. We utilized the aforementioned glycine-capped hexanuclear Ce_6O_8 cluster instead of traditionally used cerium ammonium nitrate, given the cluster's lowered reduction potential which can circumvent the formation of $Ce(HCOO)_3$ in the DMF synthesis.[42,48,49] We introduced equivalencies of a targeted modulator in a solvothermal synthesis that reacted overnight and utilized powder X-ray diffraction (PXRD) for preliminary structural characterization. Through PXRD, we observed an

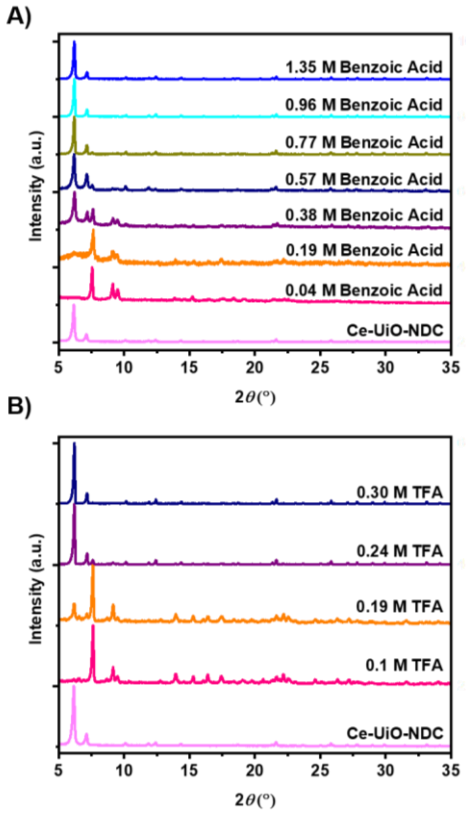

Figure 2. Stacked PXRD patterns of targeted synthesis of Ce-UiO-NDC using A) benzoic acid or B) trifluoroacetic acid. Bottom magenta trace labeled Ce-UiO-NDC corresponds to experimentally synthesized frameworks using the procedure from ref. 24.

alternate phase at lower concentrations of both modulators, tracked through the sharp peak appearing at 7.6 2θ (Figure 2). With increasing modulator concentrations, the characteristic Ce-UiO-NDC peaks become more prominent at 6.1 and 7.1 2θ (Figure 2). Pure-phase UiO-NDC was achieved with 1.35 M of benzoic acid as the modulator while the highly acidic TFA modulator yielded a pure phase material when present in only 0.30 M. At higher modulator conditions of TFA, we did not observe further product formation. Throughout the syntheses, the resulting PXRD patterns lacked peaks characteristic of $Ce(HCOO)_3$. SEM images (Figure S1) of these initial modulator investigations showed uniform clean octahedral particles of ~500 nm were achieved with benzoic acid as a modulator with a concentration of at least 1 M. However, at ~ 0.8 M, smaller octahedral particles of 200 nm were observed with several larger particles of about 500 nm interspersed (Figure S1). Alternatively, TFA modulated synthesis showed deformed octahedral particles of inconsistent size (Figure S1).

Intrigued by the alternative phase detected in both modulated syntheses at low concentrations, we utilized single crystal X-ray diffraction (SC-XRD) to identify the alternative structure appearing at lower modulator concentrations. A novel mononuclear Ce(III) chain MOF, comprised of 3 crystallographically distinct Ce atoms connected through naphthalene dicarboxylic acid was isolated, referred to as NU-350. NU-350 crystallized into the *P*-1 space group with a = 13.2389(6) Å, b = 13.3168(7) Å, c = 19.909(1) Å, α = 71. 557(4)°, β = 74.917(4)°, and γ = 75.843(3)°. Similar to a Ce^{3+} chain MOF also based on naphthalene carboxylate reported by Bonino and co-workers (Figure S5), we observed the coordination of DMF to the framework.[54] Interestingly, a series of three crystallographically distinct nodes repeated throughout the framework. Ce1 features 2 DMF, 4 monodentate NDC, and 1 chelating NDC that altogether

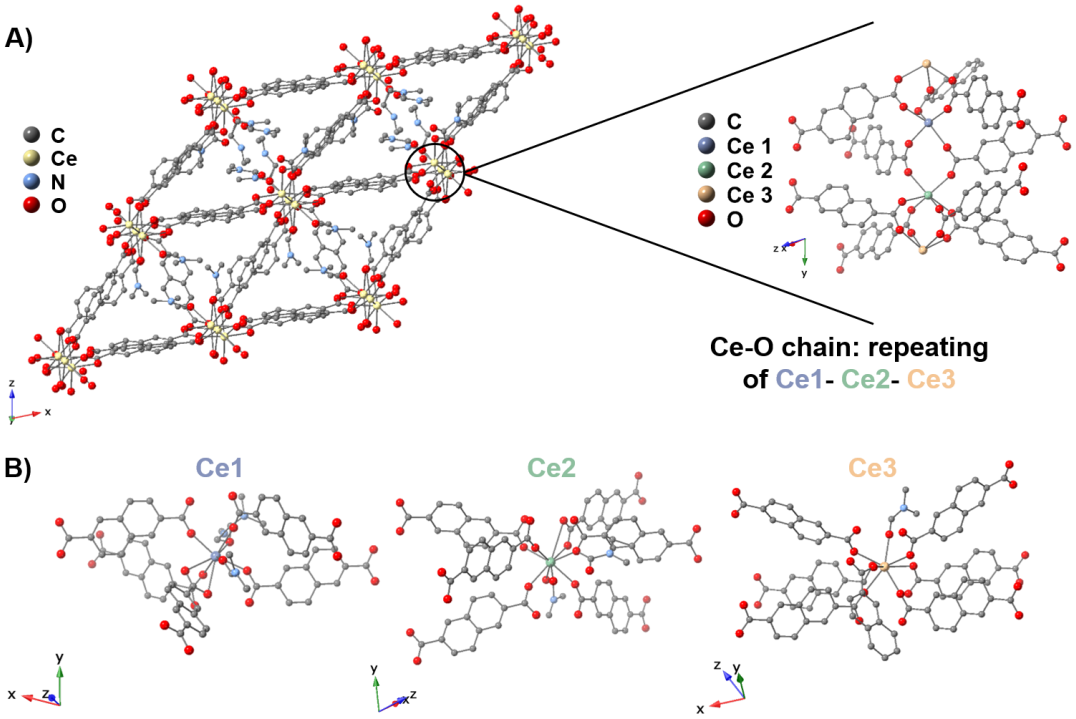

Figure 3. A) View of NU-350 viewed along crystallographic *b* axis with three crystallographically unique Ce nodes. B) Unique coordination of each Ce-based node.

comprise the CeO_8 polyhedron. Additionally, Ce2 contains 1.5 DMF, 4.5 monodentate NDC, 1 chelating NDC, and 1 OH/H_2O on the CeO_9 polyhedron. Lastly, the coordination of 1 DMF and 7 monodentate NDC moieties to Ce3 formed another CeO_8 polyhedron. X-ray photoelectron spectroscopy (XPS) confirmed the Ce^{3+} oxidation state (Figure S4) Thus, in addition to prior work documenting deleterious formation of $Ce(HCOO)_3$ in solvothermal Ce_6- MOF syntheses, these findings demonstrate the favorability of Ce^{3+} extended networks when framework modulation is low. We infer that reaction conditions hydrolyzed the Ce_6 node to yield the individual Ce atoms in solution yet increasing monocarboxylate capping agents in solution stabilized the Ce_6 node. Thus,

it is suggested that modulators limited the reduction of Ce^{4+} needed to access NU-350 which presents a new, intriguing role in modulating self-assembly for MOFs with highly redox active inorganic nodes.

With insights gained from modulator concentration effects on structure and growth, we developed a finetuned Ce-UiO-NDC synthesis to probe bulk porosity utilizing benzoic acid as a modulator. To determine if our insights of controlled Ce-UiO-NDC MOF were transferable within the Ce-UiO MOF family, bulk procedures to synthesize Ce-UiO-66 were additionally developed. PXRD patterns overlaid with their simulated Zr analogues demonstrated good agreement in phase purity (Figure 4A/B). A likely increase in unit cell parameters is consistent with the shifting of Ce experimental peaks to lower 2θ, attributed to the larger in lattice constants consistent with an anticipated larger unit cell of the Ce MOFs likely due to larger Ce-O bond distances as compared to Zr-O.[55] In addition to probing bulk crystallinity, N_2 physisorption isothermal measurements were conducted at 77 K and are consistent with a microporous material. BET area was calculated as 965 and 1265 m^2/g for Ce-UiO-66 and Ce-UiO-NDC, respectively (Figure 4C/D). Non-local density functional theory pore size distributions were calculated using a carbon-slit model and N_2 kernel to show pore sizes ~ 10 Å. Thermogravimetric analyses probed the defects present in the materials (Figure S6). Increasing modulator concentration to ~1.5 M under the fine-tuned bulk synthesis of Ce-UiO-NDC resulted in an increase of particle size to ~ 1 μm (Figure 4E) as compared to our preliminary modulation conditions. Pure octahedral morphology particles of ~600 nm Ce-UiO-66 were observed with SEM utilizing benzoic acid as a modulator (Figure 4F).

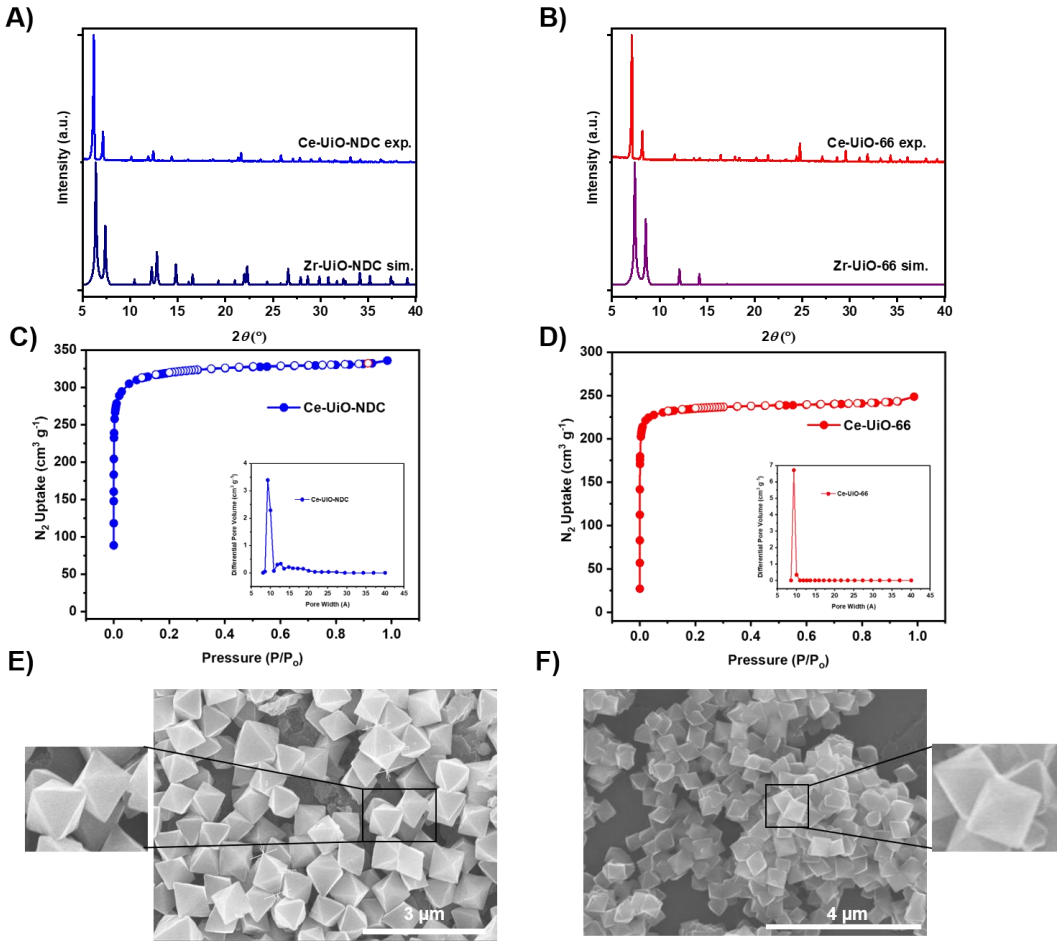

Figure 4. A/B) Experimental PXRDs of Ce-UiO-NDC and Ce-UiO-66 overlaid with simulated Zr-UiO-NDC and Zr-UiO-66, C/D) N_2 physisorption isotherms of Ce-UiO-NDC and Ce-UiO-66 with respective insets of NLDFT calculated pore size distributions. D/E) SEM images of Ce-UiO-NDC and Ce-UiO-66 respectively.

Beyond SEM imaging that provided critical insights of particle morphology and size uniformity, we utilized high-resolution transmission electron microscopy (HRTEM), a technique that allows for the direct visualization of crystalline structures and consequently provides direct proof of the structures. After exposure to low electron dose conditions, HRTEM can be utilized to specifically image smaller sized MOF particles within a few hundred nanometers, while confirming their crystallinity and nanostructures. Therefore, we elected to utilize HRTEM to directly probe the ~ 200 nm Ce-UiO-NDC particles synthesized in the initial modulator

concentration screenings. For a particle tilted on its [110] zone axis, lattice fringes of (111) and (002) planes were identified from fast Fourier transform (FFT) (Figure 5).

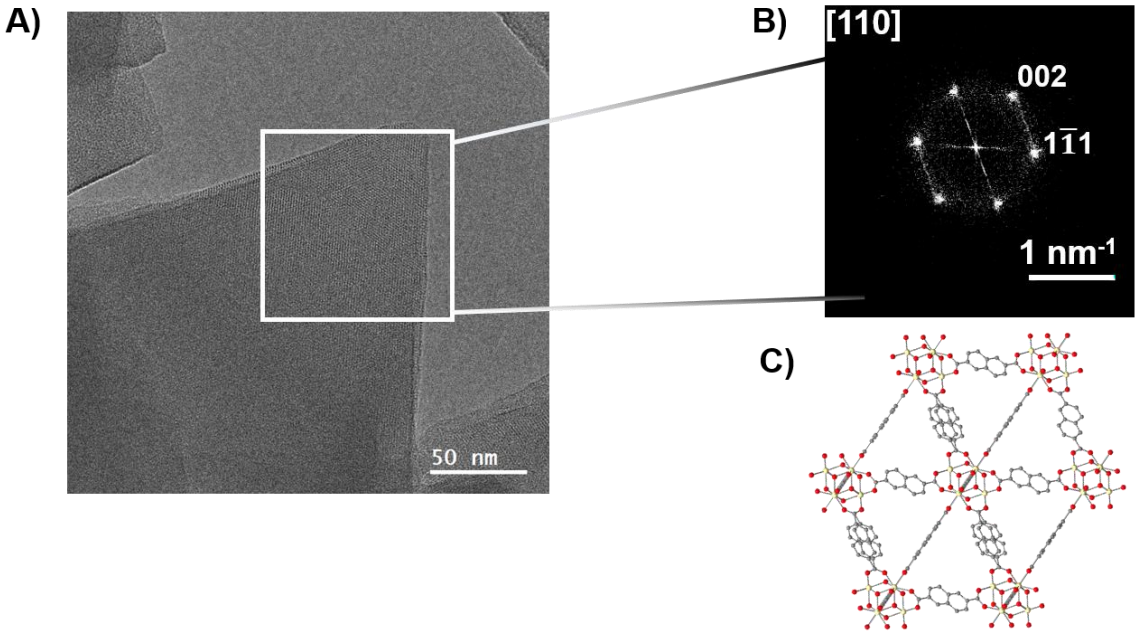

Figure 5. A) HRTEM image of Ce-UiO-NDC along [110] zone axis. B) FFT of the image inside the white square, cropped at the predominant lattice fringes. C) Simulated view of [110] plane of Ce-UiO-NDC. C, grey; O, red; Ce, pale yellow. H atoms are omitted for clarity.

Conclusions: In this work, we investigated two different modulators, benzoic acid and trifluoroacetic acid, on the crystal growth and structure of Ce-based MOFs. Through varying modulator concentration, we identified two pure-phase products: Ce-UiO-NDC and a mononuclear Ce chain MOF linked through NDC linkers (NU-350). Both modulators similarly affected MOF structure; specifically, an increase in modulator concentration resulted in both pure-phase Ce-UiO-NDC as compared to NU-350 accessed at lower modulator conditions. However, benzoic acid provided higher particle size uniformity and pure phase octahedral particles through SEM imaging. Modulator trends developed within Ce-UiO-NDC were transferable for the synthesis of pure-phase Ce-UiO-66 with octahedral particles. HRTEM imaging observed a single crystalline domain within Ce-UiO-NDC. This study provides mechanistic insights behind the

formation of cerium MOFs while also providing a strategy for accessing highly controlled MOF particles useful for further MOF investigations. The specific observation of modulators preventing the reduction of the Ce node suggests a new role of modulators in the self-assembly of redox active metals in MOF syntheses.

Acknowledgements:

Authors gratefully acknowledge the financial support from Northwestern University Institute for Catalysis in Energy Processes (ICEP), funded by the DOE, Office of Basic Energy Sciences (Award Number DE-FG02-03ER15457) and from the Army Research Office (Grant W911NF1910340). M.C.W. is supported by the NSF Graduate Research Fellowship under grant DGE-1842165. Use was made of the IMSERC X-ray facility at Northwestern University, which has received support from the Soft and Hybrid Nanotechnology Experimental (SHyNE) Resource (NSF ECCS-1542205), the State of Illinois, and the International Institute for Nanotechnology (IIN). This work made use of the EPIC facility of Northwestern University's NUANCE Center, which has received support from the SHyNE Resource (NSF ECCS-1542205), the IIN, and Northwestern's MRSEC program (NSF DMR-1720139). O.K.F. and N.C.G. gratefully acknowledge support from National Science Foundation's MRSEC program (grant number NSF DMR-1720139).

1 O. M. Yaghi, M. O'Keeffe, N. W. Ockwig, H. K. Chae, M. Eddaoudi and J. Kim, *Nature*, 2003, **423**, 705–714.

2 G. Akiyama, R. Matsuda, H. Sato, M. Takata and S. Kitagawa, *Adv. Mater.*, 2011, **23**,

3294–3297.

3 H.-C. Zhou, J. R. Long and O. M. Yaghi, *Chem. Rev.*, 2012, **112**, 673–674.

4 H. Li, M. Eddaoudi, M. O'Keeffe and O. M. Yaghi, *Nature*, 1999, **402**, 276.

5 J. Lee, O. K. Farha, J. Roberts, K. A. Scheidt, S. T. Nguyen and J. T. Hupp, *Chem. Soc. Rev.*, 2009, **38**, 1450–1459.

6 C. Wang, B. An and W. Lin, *ACS Catal.*, 2019, **9**, 130–146.

7 D. Yang and B. C. Gates, *ACS Catal.*, 2019, **9**, 1779–1798.

8 C. O. Audu, H. G. T. Nguyen, C. Y. Chang, M. J. Katz, L. Mao, O. K. Farha, J. T. Hupp and S. T. Nguyen, *Chem. Sci.*, 2016, **7**, 6492–6498.

9 R. J. Drout, K. Otake, A. J. Howarth, T. Islamoglu, L. Zhu, C. Xiao, S. Wang and O. K. Farha, *Chem. Mater.*, 2018, **30**, 1277–1284.

10 I. Abánades Lázaro, S. Haddad, S. Sacca, C. Orellana-Tavra, D. Fairen-Jimenez and R. S. Forgan, *Chem*, 2017, **2**, 561–578.

11 Y. Chen, P. Li, J. A. Modica, R. J. Drout and O. K. Farha, *J. Am. Chem. Soc.*, 2018, **140**, 5678–5681.

12 J. A. Mason, J. Oktawiec, M. K. Taylor, M. R. Hudson, J. Rodriguez, J. E. Bachman, M. I. Gonzalez, A. Cervellino, A. Guagliardi, C. M. Brown, P. L. Llewellyn, N. Masciocchi and J. R. Long, *Nature*, 2015, **527**, 357.

13 X. Cui, K. Chen, H. Xing, Q. Yang, R. Krishna, Z. Bao, H. Wu, W. Zhou, X. Dong, Y. Han, B. Li, Q. Ren, M. J. Zaworotko and B. Chen, *Science*, 2016, **353**, 141 – 144.

14 T. Islamoglu, Z. Chen, M. C. Wasson, C. T. Buru, K. O. Kirlikovali, U. Afrin, M. R. Mian and O. K. Farha, *Chem. Rev.*, 2020, DOI:10.1021/acs.chemrev.9b00828.

15 L. E. Kreno, K. Leong, O. K. Farha, M. Allendorf, R. P. Van Duyne and J. T. Hupp, *Chem. Rev.*, 2012, **112**, 1105–1125.

16 Z. Hu, B. J. Deibert and J. Li, *Chem. Soc. Rev.*, 2014, **43**, 5815–5840.

17 R. Jin, C. Zeng, M. Zhou and Y. Chen, *Chem. Rev.*, 2016, 116, 10346–10413.

18 G. Nickerl, I. Senkovska and S. Kaskel, *Chem. Commun.*, 2015, **51**, 2280–2282.

19 M. C. Wasson, C. T. Buru, Z. Chen, T. Islamoglu and O. K. Farha, *Appl. Catal. A Gen.*, 2019, 586.

20 O. M. Yaghi, *ACS Cent. Sci.*, 2019, 5, 1295–1300.

21 S. Yuan, J.-S. Qin, C. T. Lollar and H.-C. Zhou, *ACS Cent. Sci.*, 2018, **4**, 440–450.

22 J. H. Cavka, S. Jakobsen, U. Olsbye, N. Guillou, C. Lamberti, S. Bordiga and K. P. Lillerud, *J. Am. Chem. Soc.*, 2008, **130**, 13850–13851.

23 M. H. Beyzavi, N. A. Vermeulen, A. J. Howarth, S. Tussupbayev, A. B. League, N. M. Schweitzer, J. R. Gallagher, A. E. Platero-Prats, N. Hafezi, A. A. Sarjeant, J. T. Miller, K. W. Chapman, J. F. Stoddart, C. J. Cramer, J. T. Hupp and O. K. Farha, *J. Am. Chem. Soc.*, 2015, **137**, 13624–13631.

24 M. Lammert, M. T. Wharmby, S. Smolders, B. Bueken, A. Lieb, K. A. Lomachenko, D. De Vos and N. Stock, *Chem. Commun.*, 2015, **51**, 12578–12581.

25 Z. Chen, S. L. Hanna, L. R. Redfern, D. Alezi, T. Islamoglu and O. K. Farha, *Coord.*

Chem. Rev., 2019, **386**, 32–49.

26 J. E. Mondloch, W. Bury, D. Fairen-Jimenez, S. Kwon, E. J. DeMarco, M. H. Weston, A. A. Sarjeant, S. T. Nguyen, P. C. Stair, R. Q. Snurr, O. K. Farha and J. T. Hupp, *J. Am. Chem. Soc.*, 2013, **135**, 10294–10297.

27 H.-L. Jiang, D. Feng, K. Wang, Z.-Y. Gu, Z. Wei, Y.-P. Chen and H.-C. Zhou, *J. Am. Chem. Soc.*, 2013, **135**, 13934–13938.

28 J. E. Mondloch, M. J. Katz, W. C. Isley III, P. Ghosh, P. Liao, W. Bury, G. W. Wagner, M. G. Hall, J. B. DeCoste, G. W. Peterson, R. Q. Snurr, C. J. Cramer, J. T. Hupp and O. K. Farha, *Nat. Mater.*, 2015, **14**, 512.

29 L. R. Redfern, L. Robison, M. C. Wasson, S. Goswami, J. Lyu, T. Islamoglu, K. W. Chapman and O. K. Farha, *J. Am. Chem. Soc.*, 2019, **141**, 4365–4371.

30 H. Furukawa, F. Gandara, Y.-B. Zhang, J. Jiang, W. L. Queen, M. R. Hudson and O. M. Yaghi, *J. Am. Chem. Soc.*, 2014, **136**, 4369–4381.

31 S. Krause, V. Bon, U. Stoeck, I. Senkovska, D. M. Többens, D. Wallacher and S. Kaskel, *Angew. Chemie Int. Ed.*, 2017, **56**, 10676–10680.

32 A. Schaate, P. Roy, A. Godt, J. Lippke, F. Waltz, M. Wiebcke and P. Behrens, *Chem. – A Eur. J.*, 2011, **17**, 6643–6651.

33 T. Tsuruoka, S. Furukawa, Y. Takashima, K. Yoshida, S. Isoda and S. Kitagawa, *Angew. Chem. Int. Ed.*, 2009, **48**, 4739–4743.

34 T. Islamoglu, K. Otake, P. Li, C. T. Buru, A. W. Peters, I. Akpinar, S. J. Garibay and O. K. Farha, *CrystEngComm*, 2018, **20**, 5913-5918.

35 W. Morris, S. Wang, D. Cho, E. Auyeung, P. Li, O. K. Farha and C. A. Mirkin, *ACS Appl. Mater. Interfaces*, 2017, **9**, 33413–33418.

36 S. L. Griffin, M. L. Briuglia, J. H. ter Horst and R. S. Forgan, *Chem. – A Eur. J.*, 2020, **26**, 6910–6918.

37 R. J. Marshall, C. L. Hobday, C. F. Murphie, S. L. Griffin, C. A. Morrison, S. A. Moggach and R. S. Forgan, *J. Mater. Chem. A*, 2016, **4**, 6955–6963.

38 G. Zahn, P. Zerner, J. Lippke, F. L. Kempf, S. Lilienthal, C. A. Schröder, A. M. Schneider and P. Behrens, *CrystEngComm*, 2014, **16**, 9198–9207.

39 R. S. Forgan, *Chem. Sci.*, 2020, 11, 4546–4562.

40 T. Islamoglu, A. Atilgan, S.-Y. Moon, G. W. Peterson, J. B. DeCoste, M. Hall, J. T. Hupp and O. K. Farha, *Chem. Mater.*, 2017, **29**, 2672–2675.

41 M. Lammert, H. Reinsch, C. A. Murray, M. T. Wharmby, H. Terraschke and N. Stock, *Dalt. Trans.*, 2016, **45**, 18822–18826.

42 N. Heidenreich, S. Waitschat and H. Reinsch, *Zeitschrift für Anorg. und Allg. Chemie*, 2018, **644**, 1826–1831.

43 B. Wang, W. Liu, W. Zhang and J. Liu, *Nano Res.*, 2017, **10**, 3826–3835.

44 G. C. Shearer, S. Chavan, S. Bordiga, S. Svelle, U. Olsbye and K. P. Lillerud, *Chem. Mater.*, 2016, **28**, 3749–3761.

45 W. Zhou and H. F. Greer, *Eur. J. Inorg. Chem.*, 2016, **2016**, 941–950.

46 U. Ramamurty and J. Il Jang, *CrystEngComm*, 2014, **16**, 12–23.

47 M. Campanelli, T. Del Giacco, F. De Angelis, E. Mosconi, M. Taddei, F. Marmottini, R. D'Amato and F. Costantino, *ACS Appl. Mater. Interfaces*, 2019, **11**, 45031–45037.

48 S. Smolders, A. Struyf, H. Reinsch, B. Bueken, T. Rhauderwiek, L. Mintrop, P. Kurz, N. Stock and D. E. De Vos, *Chem. Commun.*, 2018, **54**, 876–879.

49 S. L. Estes, M. R. Antonio and L. Soderholm, *J. Phys. Chem. C*, 2016, **120**, 5810–5818.

50 P. Zhao, F. Qin, Z. Huang, C. Sun, W. Shen and H. Xu, *Chem. Eng. J.*, 2018, **349**, 72–81.

51 J. Zhou, H. Liu, Y. Lin, C. Zhou and A. Huang, *Microporous Mesoporous Mater.*, 2020, **302**, 110224.

52 J. Lyu, X. Gong, S. J. Lee, K. Gnanasekaran, X. Zhang, M. C. Wasson, X. Wang, P. Bai, X. Guo, N. C. Gianneschi and O. K. Farha, *J. Am. Chem. Soc.*, 2020, **142**, 4609–4615.

53 G. Ayoub, T. Islamoglu, S. Goswami, T. Friščić and O. K. Farha, *ACS Appl. Mater. Interfaces*, 2019, **11**, 15788–15794.

54 C. Atzori, K. A. Lomachenko, S. Øien-ØDegaard, C. Lamberti, N. Stock, C. Barolo and F. Bonino, *Cryst. Growth Des.*, 2019, **19**, 787–796.

55 Y. Nagai, T. Yamamoto, T. Tanaka, S. Yoshida, T. Nonaka, T. Okamoto, A. Suda and M. Sugiura, in *Topics in Catalysis*, Springer, 2008, vol. 47, pp. 137–147.

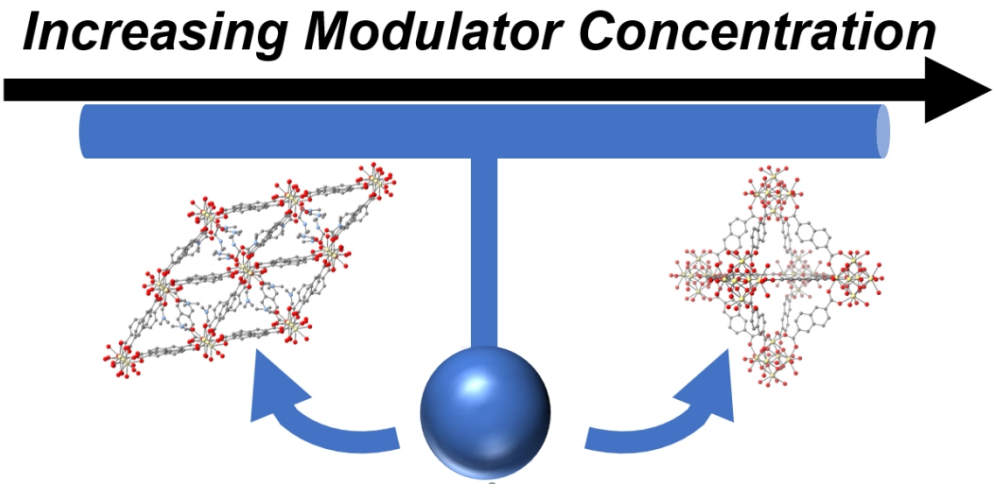
Increasing Modulator Concentration